A&A 467, 501–508 (2007)
DOI: 10.1051/0004-6361:20066226

Astronomy & Astrophysics

SWIFT observations of TeV BL Lacertae objects

A. Tramacere[1], P. Giommi[2], E. Massaro[1,2], M. Perri[2], R. Nesci[1], S. Colafrancesco[3], G. Tagliaferri[4], G. Chincarini[4], A. Falcone[5], D. N. Burrows[5], P. Roming[5], M. McMath Chester[5], and N. Gehrels[6]

[1] Dipartimento di Fisica, Università La Sapienza, Piazzale A. Moro 2, 00185 Roma, Italy
[2] ASI Science Data Center, ESRIN, via G. Galilei, 00044 Frascati, Italy
e-mail: paolo.giommi@asdc.asi.it
[3] INAF, Osservatorio Astronomico di Roma, via Frascati 33, Monteporzio Catone, Italy
[4] INAF, Osservatorio Astronomico di Brera, via Bianchi 46, 23807 Merate, Italy
[5] Department of Astronomy and Astrophysics, Pennsylvania State University, USA
[6] NASA-Goddard Space Flight Center, Greenbelt, Maryland, USA

Received 10 August 2006 / Accepted 8 November 2006

ABSTRACT

Context. We present the results of a set of observations of nine TeV detected BL Lac objects performed by the *XRT* and *UVOT* detectors on board the *Swift* satellite between March and December 2005.
Aims. Our main goal is the accurate measurement of the spectral shape of TeV detected BL Lacs. Particular attention was given to the presence of intrinsic spectral curvature in the X-ray band.
Methods. To perform our X-ray spectral analysis we have assumed either a log-parabolic or a simple power-law model.
Results. The X-ray data of many objects in our sample clearly show highly significant spectral curvature. However, in sources with spectral energy distribution peaked at energies lower than ∼0.1 keV the X-ray spectrum is steep and generally consistent with a power law. In most of these cases poor statistics did not allow us to obtain tight constraints on the spectral curvature. We have used *UVOT* observations to verify if X-ray spectra can be extrapolated to lower frequencies and to search for multiple emission components.
Conclusions. The results of our analysis are useful for the study of possible signatures of statistical acceleration processes predicting intrinsically curved spectra and for modelling the SED of BL Lacertae objects up to TeV energies where a corresponding curvature is likely to be present.

Key words. radiation mechanisms: non-thermal – galaxies: BL Lacertae objects: general – X-rays: galaxies

1. Introduction

All blazars detected at TeV energies are nearby High energy peaked BL Lacs (HBL), that is objects with the synchrotron peak in their Spectral Energy Distribution (SED) close to or within the X-ray band (Padovani & Giommi 1995). The simultaneous study of these sources at TeV and X-ray energies is very important to test the spectral and flux correlations predicted by emission models, in particular the Synchrotron Self Compton (SSC) scenario.

The energy distribution of the synchrotron component in the Log(νF_ν) vs. Log(ν) diagram is generally characterized by a rather smooth broad curvature which can be represented by a logarithmic parabola (e.g. Landau et al. 1986; Massaro et al. 2004a,b). In a recent work on the connection between the parameters of synchrotron and inverse Compton radiation in a SSC scenario applied to Mkn 501, Massaro et al. (2006) showed that intrinsic X-ray spectral curvature implies curved TeV spectra.

In this paper we present the results of a number of *Swift* (Gehrels et al. 2004) observations of a sample of nine TeV BL Lac objects performed between March and December 2005 using the *XRT* (Burrows et al. 2005) and *UVOT* (Roming et al. 2005) telescopes. We found that some of these objects exhibit a remarkable X-ray spectral curvature in agreement with previous *Beppo*SAX results (Massaro et al. 2004a,b; Costamante et al. 2001; Tagliaferri et al. 2003). recent analysis on *XMM*-Newton X-ray data of thirteen HBL sources (Perlman et al. 2005) also found evidence for significant intrinsic curvature.

Simultaneous optical, UV and X-ray observations are clearly very important to probe the presence of single or multiple non-thermal components in TeV BL Lacs. Under this respect *Swift* observations provide a unique opportunity for broad-band studies of this class of non-thermal sources. The present analysis is devoted to the measurement of intrinsic X-ray spectral curvature by means of new UV-X-ray observations of a sample of BL Lac objects.

2. *Swift* observations and data reduction

We present results concerning *Swift* pointings performed between March and December 2005. The satellite operated with all the instruments in data taking mode. However, here we only consider *XRT* and *UVOT* data since our sources were not detected by the high energy experiment *BAT* (Barthelmy et al. 2005). We also excluded from our analysis all *XRT* observations in which the total number of net counts was not sufficient for a reliable estimate of the spectral parameters. The log of X-ray observations is reported in Table 1.

2.1. XRT data

All the data were reduced using the *XRTDAS* software (version v1.8.0) developed at the ASI Science Data Center (ASDC) and distributed within the HEASOFT 6.0.5 package by the NASA High Energy Astrophysics Archive Research Center (HEASARC).

Table 1. *XRT* observation journal and exposures of TeV blazars.

Object	Date	Start UT h m	Exp. s	*XRT* mode
1H 1100−230	Jun. 30	00:08	8521	PC
	Jul. 13	14:19	2264	PC
	Nov. 04	20:34	1164	PC
	Nov. 14	14:47	554	PC
Mkn 421	Mar. 01	01:13	7134	WT
	Mar. 31	00.58	6958	WT
	Apr. 01	04:08	2465	WT
	Apr. 29	17:45	2126	WT
	May 03	05:04	318	WT
	Jul. 07	19:36	2775	WT
	Oct. 04	04:19	8063	WT/PC
	Nov. 06	02:49	1126	WT/PC
1ES 1218+304	Oct. 30	21:18	2013	PC
	Oct. 31	19:49	3701	PC
H 1426+428	Mar. 31	00:02	2935	WT/PC
	Apr. 02	17:59	4646	WT/PC
	Jun. 19	04:56	21373	PC
	Jun. 25	05:54	21203	WT/PC
1ES 1553+113	Apr. 20	03:37	5188	PC
	Oct. 06	01:16	10802	WT/PC
	Oct. 07	23:32	10718	WT/PC
1ES 1959+650	Apr. 19	00:21	4437	WT
PKS 2005−489	Mar. 31	00:06	2215	WT
	Apr. 05	00:38	8654	WT/PC
	Apr. 06	00:45	19246	WT/PC
PKS 2155−304	Nov. 17	19:22	1166	WT/PC
1ES 2344+514	Apr. 19	00:30	4665	PC
	May 19	16:10	4039	PC
	Dec. 03	00:10	12204	PC

The operational mode of *XRT* is automatically controlled by the on-board software that uses the appropriate CCD read-out mode to reduce or eliminate the effects of photon pile-up. When the target count-rate is higher than ≈1 cts/s the system is normally operated in Windowed Timing (WT) mode whereas the Photon Counting (PC) mode is used for fainter sources (see Burrows et al. 2005; and Hill et al. 2004, for more details on *XRT* observing modes). For our analysis we selected photons with grades in the range 0–12 for PC mode and 0–2 for WT mode; we also used default screening parameters to produce level 2 cleaned event files. In those cases where some pile-up was present in PC mode we excluded from our analysis all photons coming from internal part of the Point Spread Function (PSF). More specifically, spectral data collected in PC mode were extracted in an annular region with an outer radius of 30 pixels while the inner radius was chosen according to the prescription of Moretti et al. (2005). Spectra were binned to ensure a minimum of 20 counts per bin.

A residual feature at $E \approx 0.5$ keV, is still present in the best *XRT* calibration available at the time of writing (Campana et al. 2006). To avoid artificially high χ^2 values and possible biases in spectral parameter estimation, in accordance with the *XRT* calibration experts, we decided to exclude from our analysis the energy channels between 0.4 keV and 0.6 keV (Campana & Cusumano 2006, private communication). The corresponding background was estimated in a nearby source-free circular region having a radius of 35 pixels.

2.2. UVOT data

A variety of filter combinations and data modes are available for *UVOT* observations. For fields not including very bright stars, the most commonly-used observing procedure, consists of a sequence of exposures in six photometric bands: U, B, V and three ultraviolet. The list of all considered *UVOT* observations is given in Table 2.

Table 2. *UVOT* observation journal of TeV blazars.

Object	Date	Start UT h m	$E(B-V)$
1H 1100−230	Jun. 30	00:06	0.059
	Jul. 13	14:19	
	Nov. 04	20:34	
	Nov. 14	14:47	
H 1426+428	Mar. 30	23:59	0.012
	Apr. 02	17:58	
	Jun. 19	06:58	
	Jun. 25	05:58	
1ES 1553+113	Apr 20	03:37	0.052
	Oct. 06	01:16	
	Oct. 07	23:32	
1ES 1959+650	Apr. 19	01:03	0.177
1ES 2344+514	Apr. 19	01:12	0.216

We performed the photometric analysis using a standard tool *UVOTSOURCE* in HEASOFT 6.0.5. Counts were extracted from a 6″ radius aperture in the V, B, and U filters and from a 12″ radius aperture for the other UV filters (*UVW*1, *UVM*2, and *UVW*2), to properly take into account the wider PSF in these bandpasses. The count rate was corrected for coincidence loss and the background subtraction was performed by estimating its level in an offset region at 20″ from the source. The estimation of flux uncertainties is complex because of the possible presence of instrumental systematics (e.g. residual pile-up in the central region of the PSF) and imperfect calibration: in particular, the lack of reference stars in the UV bandpasses. In this paper we adopt the conservative approach using a fixed uncertainty of 8% for the V, B, U filters, and of 15% for the UV filters.

The correction for the interstellar reddening was obtained assuming the $E(B-V)$ values taken from NED and listed in Table 2; the fluxes were derived with the same conversion factors given in Giommi et al. (2006).

3. Spectral analysis and results

Spectral analysis was performed fixing the $N_{\rm H}$ absorbing column densities to the Galactic values and using the following two spectral models
a simple power law (PL)

$$F(E) = K\,E^{-\alpha} \tag{1}$$

and a log-parabolic law (LP)

$$F(E) = K\,E^{-(a+b\mathrm{Log}(E))}, \tag{2}$$

where a is the spectral slope (given by the log-derivative) at 1 keV and b measures the spectral curvature. An equivalent functional relationship, that can be used to obtain independent estimates of b and the peak energy ($E_{\rm p}$) in the SED ($S(E) = E^2F(E)$), is (LPS):

$$S(E) = K_{\rm S}10^{-b\ [\mathrm{Log}(E/E_{\rm p})]^2} \tag{3}$$

where $K_{\rm S} = E_{\rm p}^2F(E_{\rm p})$.

Equation (2) was used when the residuals of the best fits to a power law model showed significant systematic deviations, indicating the presence of intrinsic curvature. As an example Fig. 1

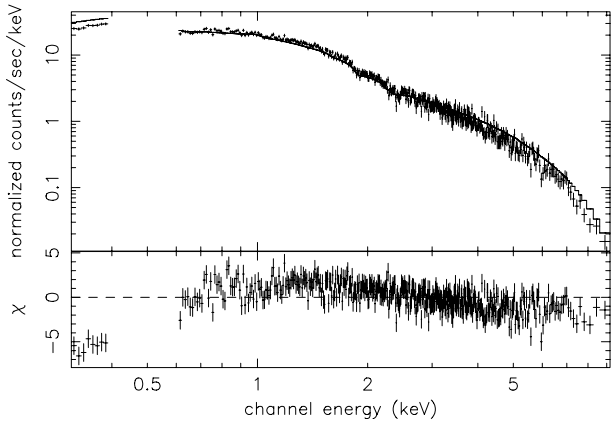

Fig. 1. *XRT* spectrum of the observation of Mkn 421 performed on 29/04/05. The systematic deviations of the best fit residuals from a simple power law and the Galactic $N_{\rm H}$ demonstrate the presence of intrinsic curvature.

shows the spectral data of Mkn 421. Such deviations from a simple power law were typically found in long exposures where the counting statistics was particularly good.

In these cases the use of the LP law significantly improved the χ^2 and eliminated the systematic deviations of the residuals.

In principle several possible curved models could give acceptable fits to the data. For this analysis we used the LP model for the following reasons: *i*) *Beppo*SAX spectral analysis of several blazars has shown that this model is a good description of the data between 0.1 keV and ∼100 keV (Massaro et al. 2004a,b; Giommi et al. 2005; Donato et al. 2005); *ii*) log-parabola is the simplest analytical law that can be used to describe continuous curvatures; in particular, it implies a linear relationship between the spectral slope and the logarithm of energy; *iii*) this spectral distribution is based on a physical interpretation in terms of statistical acceleration of the emitting particles (see Massaro et al. 2004a, 2006); *iv*) the curvature parameter allows to compare the spectral evolution of the sources in a homogeneous way. This comparison is more complex if spectral curvature is described by two or more parameters.

An alternative approach, that would probably give technically acceptable fits in the limited *XRT* energy range, is to allow $N_{\rm H}$ to be a free parameter.

We verified this possibility and found that in some sources the PL best fit with a free absorbing column gives $N_{\rm H}$ estimates well in excess of the Galactic value and variable on time scales as short as one day. Such variations are unlikely for absorbing columns distributed over large distances. Moreover, a large intrinsic absorption in the X-rays implies a strong extinction in the UV band in contrast with the *UVOT* results reported below.

A summary of the results of this spectral analysis is reported in Table 3, for the sources for which we applied the LP model (or LPS for a direct estimate of $E_{\rm p}$), and in Table 4 for the sources for which the PL gave acceptable fits. For the few observations in which very low best fit curvatures were obtained the spectral parameters are given in both Tables 3 and 4.

In the following we present our results for each source.

3.1. 1H 1100–230

At $z = 0.186$, 1H 1100−230 is one of the farthest TeV BL Lac objects. This source was observed by *Beppo*SAX twice in 1997 and 1998 and showed a stable curvature $b = 0.3 \pm 0.1$, although its flux, SED peak position, and spectral slope at 1 keV a were found to be variable. In the two states the 2–10 keV flux changed from 2.5 to 3.7×10^{-11} erg cm^{-2} s^{-1}, a moved from 1.9 ± 0.1 to 1.6 ± 0.1 and $E_{\rm p}$ from 1.5 to 4.6 keV, respectively (Giommi et al. 2005). The source was observed by HESS in 2004 and 2005 (Aharonian et al. 2006a) and its TeV spectrum, after the correction for pair production absorption, showed an intrinsic photon index close to the flat value of 1.5 when using a low intensity EBL model. Our analysis of *Swift* data shows significant spectral curvature only during the longest observation on June 30, with a value of $b = 0.40 \pm 0.06$, which is statistically consistent with those found by *Beppo*SAX and *XMM*-Newton (Perlman et al. 2005). The much shorter observation of July 13 is compatible with a low curvature spectrum, and the PL fit gave a good χ^2 (see Table 4). In the other two pointings of November 2005 the statistics were too low to allow the measurement of any spectral curvature.

The 2–10 keV flux was remarkably stable during all pointings, remaining around the value of 4×10^{-11} erg cm^{-2} s^{-1}. The source was detected by *UVOT* and the optical-UV photometry on June 30 and July 13 gives the flux values reported in Table 5. Figure 2 shows the SED of 1H 1100−230 from the IR to X-ray band, including literature measurements and *Beppo*SAX data from Giommi et al. (2005). Note the very good agreement between optical and UV data at different epochs while X-ray data show a much stronger variability. We found that the low energy extrapolation of the LP law derived only from X-rays generally fails to match UV points, and therefore we fitted simultaneously *UVOT* and *XRT* data. The new values of the spectral parameters were somewhat different from those obtained from X-ray data alone. We re-computed the χ^2 keeping a and b frozen to the new values, and found that were statistically consistent with the *XRT* data. These results are reported in Table 3 under the label UV.

3.2. Mkn 421

Mkn 421, one of the nearest BL Lac objects at $z = 0.031$, was the first extragalactic source to be detected at TeV energies (Punch et al. 1992). It shows strong variability both at X-ray and TeV energies, with time scales ranging from less than one hour to years (e.g. Gaidos et al. 1996). Spectral variability was observed in the TeV band by Krennrich et al. (2002) using the Whipple telescope in 2000–2001. These authors also discovered a correlation between flux and spectral index when averaging the observations over the whole data set. In the X-ray band Mkn 421 shows strong evidence for intrinsic spectral curvature that can be described very well by a LP law (e.g. Massaro et al. 2004a).

Mkn 421 was observed by *Swift* eight times from March to November 2005. Despite the large source flux, the last two observations were performed in PC mode causing an amount of pile-up that turned out to be too severe for a reliable analysis. Large variations of the 2–10 keV flux, by a factor of about 20, were observed from March to July when it reached the highest level of 6.7×10^{-10} erg cm^{-2} s^{-1}. In the two subsequent observations the flux decreased to $\sim 4.5 \times 10^{-10}$ erg cm^{-2} s^{-1}. In all the observations the spectrum was remarkably curved with b ranging from about 0.3 ± 0.03 to 0.46 ± 0.02; the peak energy in the SED changed between 0.1 and 0.8 keV. Three SEDs of Mkn 421 are shown in Fig. 3.

There is a wide literature on past X-ray observations of this source (e.g. Massaro et al. 2004a; Tanihata et al. 2004, and references therein). In our *XRT* observations Mkn 421 showed large flux variations that are consistent with historic data. The highest 0.2–10 keV flux measured in July 2005 is compatible with that

Table 3. Spectral parameters and fluxes of the log-parabolic model for the *XRT* observations of TeV sources.

Source/Date	N_H 10^{20} cm^{-2}	a	b	K 10^{-2}	χ^2_r/d.o.f.	E^*_p (keV)	Flux(2–10 keV) 10^{-10} erg cm^{-2} s^{-1}
1H 1100−230							
Jun. 30	5.7	1.95(0.03)	0.40 (0.06)	2.38(0.04)	0.95/121	1.15(0.09)	0.44
UV		2.01	0.15	2.30(0.03)	1.13/123	–	–
Jul. 13		2.16(0.06)	0.1 (0.1)	2.46(0.07)	0.79/70	0.3 (0.4)	0.42
UV		2.08	0.17	2.40(0.06)	0.82/72	–	
Mkn 421							
Mar. 01	1.61	2.58 (0.01)	0.31(0.03)	4.35 (0.03)	1.06/299	0.12(0.02)	0.37
Mar. 31		2.410(0.008)	0.35(0.02)	7.09 (0.04)	1.097377	0.26(0.02)	0.73
Apr. 01		2.201(0.009)	0.46(0.02)	18.7 (0.1)	0.97/396	0.60(0.02)	2.33
Apr. 29		2.095(0.008)	0.44(0.02)	25.6 (0.1)	0.97/442	0.78(0.02)	3.76
May 03		2.14 (0.03)	0.41(0.06)	15.8 (0.3)	1.16/169	0.67(0.08)	2.24
Jul. 07		2.165(0.005)	0.37(0.01)	47.61(0.01)	1.22/450	0.60(0.02)	6.74
1ES 1218+304							
Oct. 30	1.73	1.8 (0.1)	0.6 (0.2)	0.17(0.05)	1.08/32	1.5 (0.2)	0.23
Oct. 31		2.14(0.06)	0.3 (0.1)	1.12(0.04)	1.09/61	0.6 (0.2)	0.17
H 1426+428							
Mar. 31	1.38	1.96(0.06)	0.16(0.1)	0.67(0.03)	1.07/70	1.3(0.5)	0.16
Apr. 02		2.01(0.03)	0.12(0.06)	1.48(0.02)	0.95/215	0.8(0.3)	0.33
UV		1.9	0.17	1.47(0.02)	0.96/217	–	
Jun. 19		1.78(0.02)	0.34(0.03)	2.27(0.02)	0.92/300	2.0(0.1)	0.56
UV		1.84	0.16	2.20(0.02)	1.03/302	–	
Jun. 25		1.89(0.02)	0.37(0.05)	1.85(0.02)	1.15/232	1.4(0.05)	0.38
1ES 1553+113							
Apr. 20	3.67	2.25(0.05)	0.34 (0.09)	1.60(0.04)	1.14/100	0.4 (0.1)	0.21
UV		2.3	0.08	1.54(0.03)	1.21/102	–	
Oct. 0 6WT		2.20(0.02)	0.32 (0.05)	4.84(0.07)	0.98/206	0.50(0.09)	0.69
UV		2.16	0.08	4.36(0.04)	1.11/208	–	
Oct. 06 PC		2.14(0.02)	0.34 (0.05)	4.57(0.06)	0.93/229	0.61(0.08)	0.69
Oct. 08		2.17(0.02)	0.23 (0.05)	4.22(0.06)	0.89/205	0.4 (0.1)	0.67
UV		2.21	0.08	4.12(0.05)	0.93/205	–	
1ES 1959+650							
Apr. 19	10.0	2.09 (0.02)	0.46(0.03)	8.15 (0.06)	0.98/282	0.79(0.05)	1.17
UV		2.21	0.22	8.21 (0.05)	1.21/284	–	
PKS 2005−489							
Mar. 31	5.08	2.90(0.03)	0.27 (0.09)	1.85(0.04)	0.94/126	–	0.11
PKS 2155−304							
Nov. 17	1.69	2.70(0.05)	0.3 (0.1)	2.26(0.08)	0.62/53	0.1(0.3)	0.16

* Estimated from the LPS spectral model.

reached in April 2000 (Massaro et al. 2004a). The curvature is instead more pronounced with a value of about 0.37 compared to the April 2000 value of $b \simeq 0.2$. Typical E_p values in July 2005 are different from those observed in April 2000 when E_p was about 3 keV. The detailed description of the X-ray spectral evolution is a complex topic; an exhaustive analysis will be presented in a future paper (Tramacere et al. 2007).

3.3. 1ES 1218+304

This source ($z = 0.182$) has been detected at TeV energies in January 2005 by *MAGIC* (Albert et al. 2006). The TeV spectrum is described by a power law with a steep photon index of about 3, very similar to that found for PKS 2005−489 by HESS (Aharonian et al. 2005a). *Beppo*SAX observed 1ES 1218+304 on 12 July 1999 and found a curvature $b = 0.37 \pm 0.03$ and a flux about 1.5×10^{-11} erg cm^{-2} s^{-1} (Giommi et al. 2005).

Swift observed this object two times in October 2005 finding a flux level similar to that observed by *Beppo*SAX. The statistics were too low and did not allow us to measure the spectral curvature with an acceptable significance. PL best fits indicate a variation of the photon index and a flux decrease of about 35%.

3.4. H 1426+428

H 1426+428 is one of the most extreme HBL objects: it was observed in February 1999 by *Beppo*SAX and showed a flat power law spectrum ($\alpha_X = 0.92 \pm 0.04$) which placed the synchrotron peak at energies lager than ∼100 keV (Costamante et al. 2001) similarly to the cases of Mkn 501 and 1ES 2344+514 in high states. At TeV energies it was observed by the CAT telescope in 1998–2000 (Djannati-Ataj et al. 2002). No significant evidence of spectral variability was found (Aharonian et al. 2002). Blustin et al. (2004) investigated the presence of intrinsic absorbers using the High Resolution Reflecting Grating Spectrometer (RGS) of *XMM*-Newton and found no evidence for broad absorption features nor for narrow emission or absorption lines. H 1426+428 was also observed in the 3–24 keV band by *RXTE* in 2002 when it showed significant variability both in flux and spectra (Falcone et. al 2004). In some cases these authors observed a spectral index so hard to imply a synchrotron peak energy in excess of ∼100 keV while on other occasions the peak was in the 2.9–24 keV band.

Swift observed this source four times (see Table 1). We fixed N_H to the Galactic value of 1.38×10^{20} cm^{-2}. When N_H was allowed to be a free parameter its best fit value was always

Table 4. Spectral parameters and fluxes of the power-law model for the *XRT* observations of TeV sources.

Source/Date	N_H 10^{20} cm^{-2}	α	K 10^{-2}	χ^2_r/d.o.f. PL	$P(F$-test)	Flux(2–10 keV) 10^{-10} erg cm^{-2} s^{-1}
1H 1100−230						
Jul. 13	5.7	2.03(0.04)	2.46(0.07)	0.81/71	0.187	0.44
Nov. 04		2.15(0.07)	2.0(0.1)	1.10/25		0.42
Nov. 14		2.1(0.1)	1.6(0.1)	1.13/15		0.41
1ES 1218+304						
Oct. 30	1.73	2.00(0.06)	1.11(0.05)	1.25/33	0.032	0.29
Oct. 31		2.23(0.04)	1.06(0.03)	1.20/62	0.016	0.19
H 1426+428						
Mar. 31	1.38	2.01(0.05)	0.66(0.02)	1.08/71	0.421	0.17
Apr. 02		2.05(0.02)	1.45(0.03)	0.97/216	0.03	0.35
PKS 2005−489						
Apr. 05	5.08	3.16(0.02)	1.19(0.04)	0.84/200	0.06	0.06
Apr. 06		3.05(0.02)	0.99(0.02)	0.82/217	0.06	0.06
1ES 2344+514						
Apr. 19	16.3	2.35(0.06)	0.74(0.03)	0.68/48		0.11
May 19		2.18(0.08)	0.67(0.05)	0.73/27		0.13
Dec. 12		2.32(0.05)	0.60(0.25)	0.83/65		0.09

Table 5. Dereddened fluxes (in mJy) in the *UVOT* bandpasses.

Object	Date	F_V	F_B	F_U	F_{UVW1}	F_{UVM2}	F_{UVW2}
1H 1100−230	Jun. 30	0.94	0.71	0.64	0.49	0.50	0.40
	Jul. 13						
H 1426+428	Apr. 02	0.79	0.40	0.29	0.21	0.20	0.21
	Jun. 19	0.84	0.50	0.32	0.26	0.24	0.24
1ES 1553+113	Apr. 20	8.0	7.1	6.3	4.0	3.6	3.1
	Oct. 06				6.6	6.0	5.7
	Oct. 08				6.9	6.3	5.9
1ES 1959+650	Apr. 19	4.9	3.6	3.1	2.2	2.5	1.9
1ES 2344+514	Apr. 19	4.6	2.2	1.2	0.8	0.7	0.6

consistent with the Galactic value. We found significant evidence for intrinsic curvature in two cases out of four: on June 19 the source showed a curvature parameter $b = 0.34 \pm 0.03$ with $E_p = 2.0 \pm 0.1$ keV, and on June 25 b was 0.37 ± 0.05 and E_p moved to 1.40 ± 0.05 keV. The observation of 31 March 2005 is instead consistent with a PL spectrum with a photon index $\alpha = 2.01 \pm 0.05$; the F-test probability of about 0.4 for the LP does not allow us to distinguish between the two spectral models. In this observation the statistics were not good enough to measure the position of the peak and we cannot exclude that the SED could peak above ∼10 keV. In fact, our fits are also consistent with a spectrum with a curvature of about 0.1–0.2 and the peak around 1–2 keV. The presence of residual systematic effects in the instrument's effective area below 2 keV, combined with N_H absorption does not allow us to make any firm conclusion.

The observation of April 2 is similar to that of March 31 but with better statistics. In this case the source was observed both in PC and WT mode. Due to the low number of counts collected in PC mode, we used the summed signal of the two modes. We estimated a curvature of 0.12 ± 0.06 for the LP fit and a photon index of 2.05 ± 0.02 for PL fit. The low value of the F-test probability (see Tab. 4.) suggests that the curved model could give a better description of the data. In this case the peak position derived by a LPS model was 0.8 ± 0.3 keV.

A better determination of the SED is obtained when *UVOT* data are taken into account (see Fig. 4). Note that the optical photometric points (V and B) are dominated by the flux from the host galaxy and that the non-thermal UV flux of H 1426+428 remained substantially stable at variance with the X-ray flux.

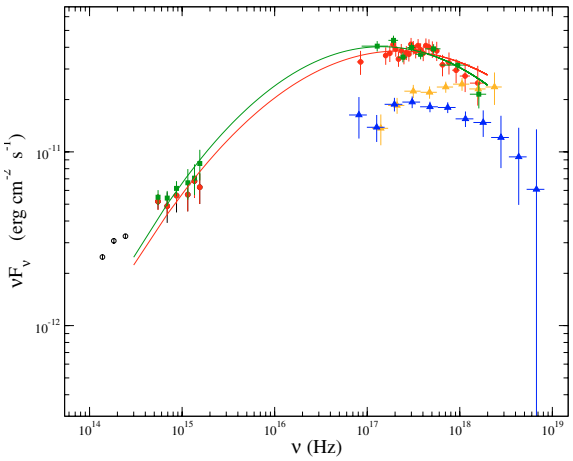

Fig. 2. Spectral Energy Distributions of 1H 1100−230 derived from *XRT* and *UVOT* observations on 30 June 2005 (filled circles) and on 13 July 2005 (filled squares). For comparison we plotted also *Beppo*SAX data (triangles) and IR photometric points from 2MASS (open circles). Dashed lines correspond to simultaneous *XRT* UV-*UVOT* fit. X-ray open triangles correspond to the *Beppo*SAX observations performed on 4 January 1997 and 19 June 1998).

Therefore, a simultaneous fit in these two bands is not straightforward.

In the observation of June 19 we found that LP model can give a good description of the data from UV to the X-rays. We performed a fit on both *UVOT* and *XRT* data with a LP (solid line in Fig. 4) and obtained spectral parameters significantly different from those obtained fitting only *XRT* data (dashed line): the new values are reported in Table 3 with the label UV. On April 02 only a single LP can match approximately both X-ray and UV points: in this case we obtained $b = 0.17$, consistent with that found for only *XRT* data (0.12 ± 0.06) within the statistical errors. The χ^2 of simultaneous *UVOT* -*XRT* fits are also very satisfactory for both observations, confirming that the addition of UV data does not produce inconsistencies. Note, however, that the lowest energy *XRT* point in the June 19 observation lies significantly below the LP spectrum and is nearly coincident with that of the other pointing. We do not have a simple explanation for this discrepancy: it could just be a statistical fluctuation, but

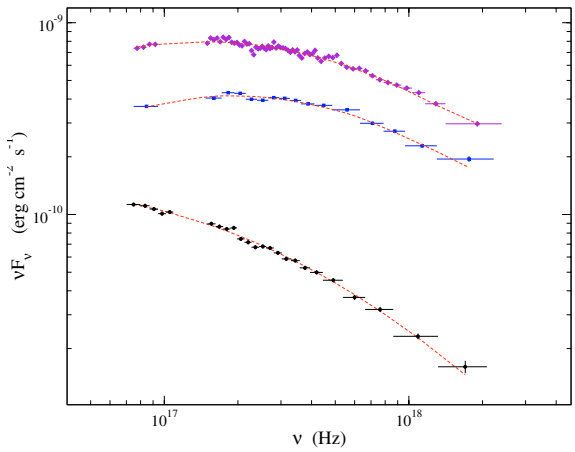

Fig. 3. Spectral Energy Distributions of Mkn 421 in the *XRT* energy range in three different brightness states observed on March 01 (bottom), April 29 (centre), and July 7 2005 (top).

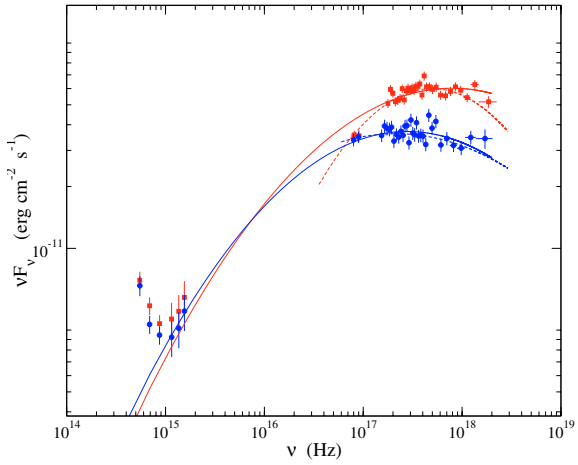

Fig. 4. Spectral Energy Distributions of H 1426+428 in the *XRT UVOT* energy range in two different brightness states observed on 19 June (squares) and 02 April (circles) 2005. Dashed lines correspond to *XRT* data fit. Solid lines correspond to simultaneous *XRT UVOT* (UV bands only) data fit.

also an indication of the emerging of another component at energies larger than ∼1 keV.

3.5. 1ES 1553+113

This object was detected for the first time at TeV energies in 2005 by HESS (Aharonian et al. 2006b). Its redshift is unknown, although Sbarufatti et al. (2006) recently derived a lower limit of $z > 0.09$. 1ES 1553+113 was observed by *Beppo*SAX on 05 February 1998 when it showed a strong spectral curvature with $b = 0.6 \pm 0.1$ and a 2–10 keV flux of 1.3×10^{-11} erg cm^{-2} s^{-1}.

We report here the results of three *Swift* observations performed in April and October 2005. In every pointing the curvature is well determined: on April 20 b was equal to 0.34 ± 0.09 and a similar value was found on October 06 (see Table 3), whereas the 2–10 keV flux (6.8×10^{-11} erg cm^{-2} s^{-1}) was more than 3 times higher than that recorded at the first epoch. Two days later, on October 07–08, the spectral curvature was slightly lower while the flux was practically unchanged.

It is interesting to note that 1ES 1553+113 is the only source in our sample with the optical/UV emission higher than that in

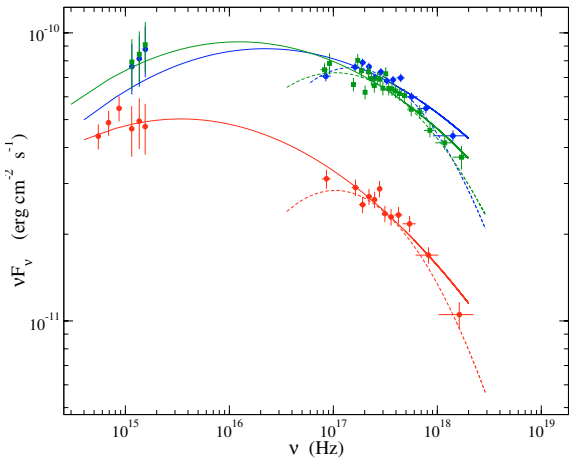

Fig. 5. Spectral Energy Distributions of 1ES 1553+113 observed on 20/04/05 (filled circles), 06/10/05 (open diamonds) and 08/10/05(filled squares), simultaneously by *XRT* and *UVOT* (UV bands only). Dashed lines correspond to *XRT* data fit. Solid lines corresponds to simultaneous *XRT* and *UVOT* (UV bands only) data fit.

the X-rays (see the SED of Fig. 5). This feature was observed in all our pointings. We plotted two best fit spectra: one for the X-ray data only (dashed lines) and the other for both *UVOT* and *XRT* points (solid lines). It is evident that when the UV points are included in the fit the resulting values of b and E_p are significantly lower: the new values of the spectral parameters are also given in Table 3 (line denoted by UV), whereas the fluxes in the *UVOT* filters are listed in Table 5. We verified that the new χ^2 values of *XRT* data computed with a and b frozen to the values coming from simultaneous UV-X points remain acceptable (see Table 3). Note in particular that the spectral curvature when UV data are taken into account is around 0.1, a value consistent with that found by Perlman et al. (2005) in high statistics *XMM*-Newton observations.

3.6. 1ES 1959+650

1ES 1959+650 ($z = 0.047$) was detected at TeV energies in 1999 (Nishiyama et al. 1999) and confirmed by Whipple (Holder 2003) and HEGRA (Horns 2003). It was observed twice by *Beppo*SAX , in September 2001 when it showed a significant spectral curvature (Tagliaferri et al. 2003). These authors used a LP law and found a value of b of about 0.4. In May 2002 1ES 1959+650 was the subject of a multi-wavelength campaign during which a strong TeV/X-ray correlation was found. There was, however, a remarkable exception of TeV flare on 4 June 2002 not associated with any X-ray activity (Krawczynski et al. 2004).

We have only one *Swift* observation of this source. In our spectral analysis we adopted the Galactic N_H value of 1.0×10^{21} cm^{-2}, although the possibility of a high intrinsic absorption cannot be excluded. We confirmed the spectral analysis with $b = 0.46 \pm 0.03$, a flux of 1.16×10^{-10} erg cm^{-2} s^{-1} and a peak energy at ∼0.8 keV. Similar spectral curvatures were also found by Perlman et al. (2005).

Recently Gutierrez et al. (2006) carried out a time resolved spectral analysis of *RXTE* observations in the 4–15 keV band and reported a curvature parameter b in the range 0.1–0.4 over a period of about four years.

As in the case of H 1426+428 and 1ES 1553+113 we found that simultaneous *UVOT-XRT* data are compatible with a LP law. In Fig. 6 (solid line), we plotted the LP broad band best fit, which

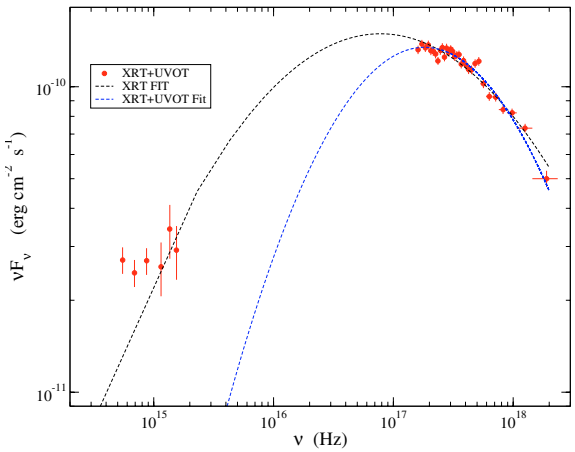

Fig. 6. Optical to X-ray SED of 1ES 1959+650 as observed on 19 April 2005 by *Swift*. Dashed line corresponds to *XRT* data fit. Solid line corresponds to simultaneous *XRT* - *UVOT* (UV bands only) data fit.

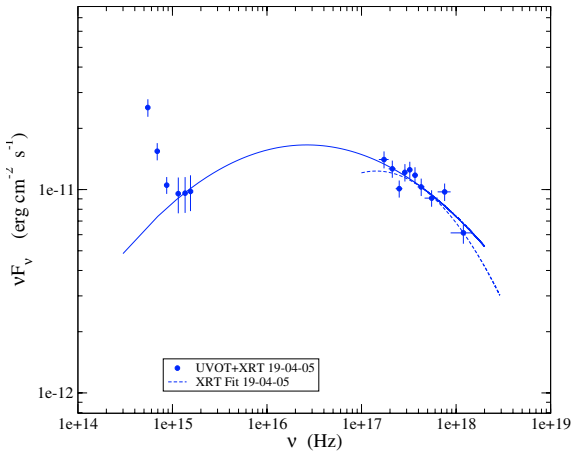

Fig. 7. Optical to X-ray SED of 1ES 2344+514 as observed on 19 April 2005 by *Swift*. Dashed line corresponds to *XRT* data fit. Solid line corresponds to simultaneous *XRT UVOT* (UV bands only) data fit.

peaks at ∼0.3 keV and has $b \simeq 0.2$. The χ^2 for the *XRT* data only is somewhat higher but is still acceptable, as for the case of previous sources.

3.7. PKS 2005–489

PKS 2005−489 ($z = 0.071$) was discovered at TeV energies by HESS (Aharonian et al. 2005a) with an integrated flux above 200 GeV of 6.9×10^{-12} erg cm^{-2}s^{-1}, corresponding to about 25% of the Crab Nebula. Past X-ray observations were performed by *Beppo*SAX in September 1996 and November 1998. The amount of spectral curvature measured during these pointings was very low and equal to 0.05 ± 0.11 and 0.12 ± 0.02, respectively. The corresponding 2–10 keV fluxes were 6×10^{-11} erg cm^{-2} s^{-1}and 1.8×10^{-10} erg cm^{-2} s^{-1}(Giommi et al. 2002).

Swift observations were performed in March and April 2005 and confirmed the low fluxes and curvatures seen by *Beppo*SAX. In March we found $b = 0.23 \pm 0.05$ and a flux of about 7×10^{-11} erg cm^{-2} s^{-1}, while in April the spectrum was consistent with a PL with a soft photon index (see Table 4). The flux computed using this spectral model is about one order of magnitude lower than that recorded in April. Such a very soft X-ray spectrum agrees well with that found in the TeV band, where HESS data showed a photon index of ≈4 (Aharonian et al. 2005a), the softest ever recorded for a BL Lac at these energies. These authors were confident that it is unlikely that this steep spectrum was the result of large absorption by EBL and argued that the X-ray spectrum must be intrinsically soft. Our analysis of *Swift* data supports this conclusion.

3.8. PKS 2155–304

PKS 2155−304 ($z = 0.117$) is one of the first BL Lac objects detected at TeV energies (Chadwick et al. 1999). It was observed by HESS in October and November 2003 and its TeV spectrum was found to be consistent with a PL with photon index of 3.32 ± 0.06 (Aharonian et al. 2005c). *Beppo*SAX observed this source three times during which the spectral curvature remained in the narrow range 0.27–0.3 whereas the flux changed from 2.5 to 8.3×10^{-11} erg cm^{-2} s^{-1}(Giommi et al. 2002).

Swift observed PKS 2155−304 in 2005 only once. The relatively poor statistics obtained during this observation were not sufficient to provide a good estimate of b (see Table 3) which was found to be similar to that measured during previous observations, despite the lower flux level. Note, however, that the value of a was significantly larger than 2 confirming the soft SED of this source.

3.9. 1ES 2344+514

This BL Lac object ($z = 0.044$) was detected at TeV energies by Catanese et al. (1998) and more recently by Schroedter et al. (2005). 1ES 2344+514 was observed by *Beppo*SAX in December 1996 and in June 1998 when it showed strong X-ray variability with large flux and spectral changes (Giommi et al. 2000).

1ES 2344+514 was observed by *Swift* on three occasions during which its 2–10 keV flux remained steady at a typical level of about 1×10^{-11} erg cm^{-2} s^{-1}. The low statistics of these observations and the high value of the Galactic column density $N_{\rm H} = 1.63\times10^{21}$ cm^{-2} do not allow us to determine the value of b with good accuracy. PL best fit parameters are given in Table 4 where we note that the photon index was always larger than 2 indicating that the peak of the SED is below 1 keV, as in the faint state reported by Giommi et al. (2000).

UVOT data are available only for the observation of April 19. The stars in the *UVW2* band image appear elongated, probably from aspect reconstruction problems, but still within the 12″ photometric radius. The results of the analysis are reported in Table 5. Because of the large Galactic extinction ($E(B-V) = 0.216$), the flux in the M2 band is strongly affected by the 2200 Å interstellar band. In addition, from the HST observation reported by Urry et al. (2000) we derived *that the host galaxy contributes for about 90% of the signal* in the V and B filters thus implying that these data are not representative of the AGN flux. In the UV filters, where the galaxian contribution is much lower, the SED appears substantially flat. In Fig. 7 the dashed line corresponds to the LP fit of the *XRT* data (not reported in Table 3 because of the low accuracy achieved in the estimation of the parameters). The solid line corresponds to the fit of *UVOT* and *XRT* data with a single LP law with curvature of about 0.15 and $E_{\rm p} \simeq 2.5$ keV.

4. Discussion

Our *Swift* observations of TeV-detected blazars strongly confirm that the SED of these sources is often curved and well approximated by a LP law with peak energy that is generally located

in the X-ray band but that can vary more than one order of magnitude.

The precise estimation of the curvature parameter is often a complex task as it may be affected by systematic and statistical uncertainties that in some cases can be very important, especially when working within a rather narrow frequency range. Under this respect, the *Swift* instrumentation offers the unique possibility of simultaneously measuring both the X-ray and UV fluxes, where the contribution from the host galaxy is generally negligible. These observations can be used to determine the SED across a frequency interval spanning over three decades thus allowing us to test whether a single emission component is sufficient to describe all data. The possible presence of multiple components was already an issue in the spectral modeling of the *Beppo*SAX observations of Mkn 421 (Massaro et al. 2004a) and Mkn 501 (Massaro et al. 2004b) where the optical and the X-ray points could not be connected in a simple way. For the sources presented in this paper we found that a single component is generally acceptable. However, there are some notable differences between different sources.

As noted in Sect. 3.5, 1ES 1553+113 is the only object with a SED dominated by UV emission. When a single LP is assumed, the synchrotron peak energy is estimated to be at frequencies lower than 10^{16} Hz.

Another interesting source is H 1426+428 which shows larger variability in the X-ray band than at UV frequencies. Note that the flux at ∼0.3 keV is also rather stable compared to that at energies larger than 1 keV, a behaviour that recalls that of Mkn 501 (Massaro et al 2004b). This finding may imply that optical/UV photons are originated from the low energy tail of the same electron population that produces X-ray photons. However, the possibility that the UV radiation is emitted by another electron population, rather stable and of lower energy, non-cospatial to the high-energy one, cannot be excluded. To discriminate between these two possibilities it is useful to study its time behavior at different wavelengths. We stress that optical and IR observations are not very useful because of the presence of a bright host galaxy that is very well detected in these bands (see Fig. 4).

Finally, note that all five sources for which the PL model gave an acceptable fit are characterized by photon indices larger than 2, corresponding to $E_{\rm p}$ values lower than 1 keV. Such steep spectra generally correspond to a low number of net counts in the *XRT* high energy channels making curvature very hard to estimate.

The shape of the X-ray spectra reflects the energy distribution of the emitting particles. The relations between the curvature of the electron spectrum and those of the Synchrotron and Inverse Compton radiation have been studied by Massaro et al. (2006). Curvature in the electron energy distribution may be the result of acceleration features like energy dependent acceleration probability (see Massaro et al. 2004a) or fluctuations in the energy gain (Kardashev 1962; Tramacere et al. 2007). Thus our X-ray analysis may be used to investigate these acceleration signatures.

The presence of intrinsic spectral curvature has a direct implication on the amount of pair production opacity due to Extragalactic Background Light (EBL), as pointed out by Massaro et al. (2006) for the case of Mkn 501 on the basis of simultaneous X-ray and TeV observations. The observed spectra are the convolution of the intrinsic shape of the IC radiation and of the γ-ray opacity. At present the amount of EBL is still uncertain (see Schroedter 2005, for a recent compilation). Upper limits on EBL density, derived assuming a PL spectrum for the TeV emission of nearby BL Lac objects, are even lower for the case of intrinsically curved IC spectra.

Acknowledgements. The authors acknowledge financial support by the Italian Space Agency (ASI) to the ASDC and to the Italian Swift team through grant I/R/039/04 and by the Phys. Dept. by Università di Roma La Sapienza. This work is sponsored at Penn State University by NASA contract NAS5-00136. We thank G. Cusumano for his support with the *XRT* calibration. We acknowledge the use of the National Extragalactic Database (NED) for the values of $E(B-V)$ listed in Table 2.

References

Aharonian, F., Akhperjanian, A., Barrio, J., et al. 2002, A&A, 384, 23
Aharonian, F., Akhperjanian, A. G., Aye, K.-M., et al. 2005a, A&A, 436, L17
Aharonian, F., Akhperjanian, A. G., Aye, K.-M., et al. 2005b, A&A, 437, 95
Aharonian, F., Akhperjanian, A. G., Bazer-Bachi, A. R., et al. 2005c, A&A, 442, 895
Aharonian, F., Akhperjanian, A. G., Bazer-Bachi, A. R., et al. 2006a, Nature, 440, 1018
Aharonian, F., Akhperjanian, A. G., Bazer-Bachi, A. R., et al. 2006b, A&A, 448, L19
Albert, J., Aliu, E., Anderhub, H., et al. 2006, ApJ, 642, L119
Barthelmy, S., Barbier, L. M., Cummings, J., et al. 2005, SSRv., 120, 95
Blustin, A. J., Page, M. J., & Branduardi-Raymont, G. 2004, A&A, 417, 61
Burrows, D., Hill, J. E., Nousek, J. A., et al. 2005, SSRv., 120, 165
Campana, S., Beardmore, A. P., Cusumano, G., Godet, O. 2006, Swift-XRT-CALDB-09
Catanese, M., Akerlof, C. W., Badran, H. M., et al. 1998, ApJ, 501, 616
Chadwick, P. M., Lyons, K., McComb, T. J. L., et al. 1999, ApJ, 513, 161
Costamante, L., Ghisellini, G., Giommi, P., et al. 2001, A&A, 371, 512
Djannati-Ataj, A., Khelifi, B., Vorobiov, S., et al. 2002, A&A, 391, L25
Donato, D., Sambruna, R. M., Gilozzi, M. 2005, A&A, 433, 1163
Draper, P. W., Gray, N., Berry, D. S. 2004, Starlink User Note, 214, 15
Dwek, E., Krennich, F. 2005, ApJ, 618, 657
Falcone, A. D., Cui, W., & Finley, J. P. 2004, ApJ, 601, 165
Gehrels, N., Chincarini, G., Giommi, P., et al. 2004, ApJ, 611, 1005
Gaidos, J. A., Akerlof, C. W., Biller, S. D., et al. 1996, Nature, 383, 319
Giommi, P., Padovani, P., Perlman, E. S. 2000, MNRAS, 317, 743
Giommi, P., Capalbi, M., et al. 2002, in Blazar Astrophysics with *BeppoSAX* and Other Observatories, 63
Giommi, P., Piranomonte, S., Perri, M., Padovani, P. 2005, A&A, 434, 385
Giommi, P., Blustin, A. J., Capalbi, M., Colafrancesco, S., et al. 2006, A&A, 456, 911
Gutierrez, K., Badran, H. M., Bradbury, S. M., et al. 2006, ApJ, 644, 742
Hill, J. E., Burrows, D. N., Nousek, J. A., et al. 2004, SPIE, 5165, 217
Holder, J. 2003, Proc. 28th Int. Cosmic Ray Conf., ICRC, 5, 2619
Horns, D. 2003, ASPC, 299, 13H
Krawczynski, H., Hughes, S. B., Horan, D., et al. 2004, ApJ, 601, 151
Krennrich, F., Bond, I. H., Bradbury, S. M., et al. 2002, ApJ, 575, L9
Landau, R., Golisch, B., Jones, T. J., et al. 1986, ApJ, 308, 78
Massaro, E., Perri, M., Giommi, P., Nesci, R. 2004a, A&A, 413, 489
Massaro, E., Perri, M., Giommi, P., et al. 2004b, A&A, 422, 103
Massaro, E., Tramacere, A., Perri, M., et al. 2006, A&A, 448, 861
Moretti, A., Campana, S., Mineo, T. et al. 2005, Proc SPIE vol 5898, 360
Nishiyama, T. 1999, Proc. 26th Int. Cosmic Ray Conf., ICRC 3, 370.
Padovani, P., Giommi, P. 1995, ApJ, 444, 567
Perlman, E. S., Madejski, G., Georganopoulos, M., et al. 2005, ApJ, 625, 727
Punch, M., Akerlof, C. W., Cawley, M. F., et al. 1992, Nature, 358, 477
Roming, P. W. A., Kennedy, T. E., Mason, K. O., et al. 2005, SSRv, 120, 143
Sbarufatti, B., Treves, A., Falomo, R., et al 2006, AJ, 132, 1
Schroedter, M., Badran, H. M., Buckley, J. H., et al. 2005, ApJ, 634, 947
Schroedter, M. 2005, ApJ, 628, 617
Tagliaferri, G., Ravasio, M., Ghisellini, G., et al. 2003, A&A, 412, 711
Tanihata, C., Kataoka, J., Takahashi, T., et al. 2004, ApJ, 601, 759
Tramacere, A., Massaro, F., Cavaliere, A. 2007, A&A, 466, 521
Urry, C. M., Scarpa, R., O'Dowd, M., et al. 2000, ApJ, 532, 816